Dynamics of relaxation at strongly interacting polymer–solid interfaces: Effects of chain architecture

Paul M. Adriani and Arup K. Chakraborty

Citation: The Journal of Chemical Physics **98**, 4263 (1993); doi: 10.1063/1.465033
View online: http://dx.doi.org/10.1063/1.465033
View Table of Contents: http://scitation.aip.org/content/aip/journal/jcp/98/5?ver=pdfcov
Published by the AIP Publishing

Dynamics of relaxation at strongly interacting polymer–solid interfaces: Effects of chain architecture

Paul M. Adriani and Arup K. Chakraborty[a)]
Center for Advanced Materials, Lawrence Berkeley Laboratory, Berkeley, California 94720 and Department of Chemical Engineering, University of California, Berkeley, California 94720

(Received 26 May 1992; accepted 3 November 1992)

The relaxation dynamics of a polymer chain strongly adsorbed to a solid surface are simulated via a kinetic Ising model that includes chain connectivity constraints (steric hindrance, rotational strain, and configurational entropy). The two polymer architectures examined consist of one or two chemisorbing functional groups per segment. In both architectures, the chemisorbed polymer chain is trapped in nonequilibrium conformational states at low temperatures, but relaxes to equilibrium at higher temperatures with stretched exponential (*KWW*) relaxation kinetics. The average relaxation time for the two pendant group architecture has a strongly non-Arrhenius temperature dependence that obeys the Vogel–Fulcher law. In contrast, average relaxation times for the one pendant group architecture cannot be described by the Vogel–Fulcher law.

I. INTRODUCTION

Polymer adsorption onto a solid surface is a problem which has attracted much attention, both for its intrinsic scientific interest and for its technological importance. This is so because the synthesis of interfaces between polymers and solid surfaces is of importance for numerous applications in the microelectronics, aerospace, automotive, food-processing, and biomedical industries, and further, elucidating the interfacial chain conformations and dynamics presents unusual scientific challenges. Polymer–solid interfaces may be divided into two broad classes. The first class is weak adsorption, or physisorption, where the polymer segments interact with the surface via dispersive interactions. The second class is strong adsorption, or chemisorption, where specific functional groups of the polymer chemisorb onto the solid surface. The polyethylene–graphite system is an example in the former class, while the interfaces between polymers and metallic substrates exemplifies the latter.

Much progress has been made toward understanding the equilibrium adsorption of weakly interacting, physisorbed polymer chains via mean-field lattice models,[1,2] scaling analyses,[3] diffusion equation methods,[4,5] renormalization group methods,[6] and Monte Carlo simulations.[7] However, only recently has there been progress in understanding the adsorption of strongly interacting, chemisorbed polymer chains [e.g. Refs. 8–18].

In these systems, the segment–surface interactions are not simple, and quantum mechanical calculations[12] have shown that the energy hypersurfaces are characterized by several configuration and orientation dependent minima that are often separated by high barriers. As a result, it has been shown[11] that the interfacial chains get trapped in local minima. Thus, the interfacial chains constitute a collection of nonequilibrium conformations. Relaxation to equilibrium conformations occurs over a range of sufficiently high temperatures, while at low temperatures the interfacial chains are kinetically constrained from acquiring the conformations corresponding to the global minimum of free energy. In a previous short communication,[14] we have shown that the dynamics that characterize the relaxation of the interfacial chains are akin to that observed for bulk glass-forming liquids. This result is consistent with the recent elegant experimental work due the Granick and coworkers[16,17] wherein similar physical phenomena are probed. In this paper, we provide a full discussion of our findings, and explore the effect of chain architecture and length on the dynamic behavior of these unique confined fluids that are composed of polymer chains interacting with strongly adsorbing solid surfaces.

This paper is organized as follows. In Sec. II we briefly review previous efforts aimed toward understanding the near-surface structure and dynamics of polymers near strongly interacting solid surfaces. This will set the stage for the work to be described in this paper. In Sec. III we describe molecular dynamics (MD) simulation for the adsorption dynamics. While MD simulations offer a fine level of detail, the computational price is such that the relevant time scales for the problem under consideration are inaccessible for long chains. In Sec. IV we describe our alternative stochastic approach, a facilitated kinetic Ising model. In Secs. V and VI we discuss the results of our calculations for two polymer architectures and various chain lengths. The discussion makes connection with experiments and we also comment on the nature of the cooperative dynamics under consideration. Some concluding remarks are made in Sec. VII.

II. BACKGROUND

Strongly interacting polymer–solid interfaces are exemplified by the interfaces between polymers and metallic substrates. In such systems, particular functional groups of the organic polymer may chemisorb onto the solid surface. These chemical interactions are not only stronger than dis-

a)Author to whom correspondence should be addressed.

persive interactions, but rather, they are also very specific. This is to say that only particular functional groups interact strongly with the surface. The interplay between the resulting strong and specific enthalpic driving forces that favor preferential adsorption of particular functional groups and the entropic constraints associated with confining chain molecules to a region adjacent to a solid surface determines the interfacial chain conformations and dynamics. The first difficulty associated with the theoretical or computational study of the systems under consideration is that unlike situations wherein the segment–surface interactions are dispersive, the nature of the interaction potentials that describe the segment–surface interactions is not known *a priori*. Once this is known, statistical mechanical methods may be employed to examine chain conformations and dynamics. Previous quantum mechanical calculations[10,19,20] employing Hartree–Fock molecular orbital theory have examined the interactions between metal atoms and model compounds for monomer units of polymers. Recent quantum mechanical calculations[12] have examined the interactions between a metal surface and short chains. These studies show that the energy hypersurfaces that characterize the interactions between monomers and dimers of poly(methyl methacrylate) (PMMA) and an aluminum surface exhibit many local minima that are often separated by energy barriers larger than k_BT. This is so because the specificity of chemisorptive interactions leads to strong orientation and conformation dependent interaction energies.

The topography of the interaction energy hypersurface has led to the idea that chain molecules interacting with solid surfaces wherein chemisorption may occur, adsorb in nonequilibrium conformations. These nonequilibrium structures arise because the segment–surface interactions are such that kinetic constraints do not allow the chains to evolve to structures corresponding to the global minimum of free energy. It is important to note that the kinetic constraints under consideration are surface induced. The interfacial chains in such a system may be viewed to be analogous to a glass-forming liquid.[11,14] In a previous communication, we presented a kinetic Ising model which showed that the dynamical behavior of these chains is characterized by frozen nonequilibrium structures at low temperatures, stretched exponential relaxation kinetics at higher temperatures, and a non-Arrhenius temperature dependence of the average relaxation times. Such glassy dynamics are not to be confused with the ideas proposed by Kremer[21] wherein adsorbed polymer layers are so densely packed near the surface that insufficient solvent remains to plasticize the polymer chains. Kremer then suggested that the polymer layer would have glassy behavior at temperatures below the bulk glass transition of the adsorbing polymer. In contrast we are considering the chemisorptive trapping of polymer chains at the surface, which has nothing to do with any possible bulk glass transition of the polymer.

The results reported in our communication are consistent with recent insightful experiments due to Johnson and *Granick*.[17] In this paper we develop our model of the cooperative dynamics that may be in the same universality class as the hierarchically constrained models proposed by Palmer, Stein, Abrahams, and Anderson.[22] The dynamical behavior of the unique confined fluids under consideration are discussed in view of the results of our calculations for two different chain architectures.

III. MOLECULAR DYNAMICS SIMULATIONS

MD simulation of polymer adsorption can only probe short time behavior of short chains due to the high computational cost of following the dynamics of each polymer and solvent atom. Furthermore, each simulation yields a single realization of the many possible nonequilibrium conformations. In order to obtain average properties for the nonequilibrium structures, initial configuration space must be efficiently sampled. Even for short chains, detailed MD studies that accomplish this are too compute intensive to be feasible. The value of MD simulation for the problem at hand is that it provides a realistic underpinning that aids in the development of a stochastic kinetic model which can then be employed for long chains and time scales. This is the sole purpose of the MD simulation studies described herein.

We employ a model system that aims to represent the important physical features of PMMA–aluminum interfaces. Quantum mechanical calculations[10,12] have shown that for this system there are two functional groups on the side chain that interact strongly with the surface, viz., the carbonyl and methoxy functional groups. The carbonyl functionality binds to the surface more strongly than the methoxy group. Our model system consists of a chain of backbone atoms wherein every other backbone atom has two pendant groups emanating from it. These pendant groups represent the methoxy and carbonyl groups, and will be referred to as the weak and strong stickers, respectively.

The computational time on a Cray X-MP/28 for simulating the adsorption to a planar interface of an octamer in a sea of 467 Lennard-Jones atoms is 1 cpu h per 100 ps simulation time. We employ standard MD simulation techniques and details of our simulations have been published previously.[11] Clearly, it is not possible to simulate long chains or long time scales via direct MD simulation. For the problem at hand, we will remedy this difficulty shortly by developing a stochastic model.

Examples of the final chain configurations obtained have been published previously.[11] Varying the initial polymer orientation or merely varying the random initial particle velocities is sufficient to yield different nonequilibrium final configurations. This validates the idea that nonequilibrium conformations constitute the interfaces under consideration.

The frequency of adsorption and desorption events at the interface provides basic information of the short time relaxation. From MD simulation the average desorption time of strong and weak stickers at 900 K is 20 and 7 ps, respectively. At 450 K the desorption time is immeasurably slow on MD time scales. We will employ the desorption frequency at 900 K to set the intrinsic time scale for our stochastic model for adsorbed chain dynamics.

The existence of nonequilibrium interfacial chain conformations raises the following intriguing questions. What are the characteristics of the dynamical behavior of the interfacial chains? How do the dynamics depend on temperature (or segment-surface energy scale), chain architecture, and chain length? We note that in order to address each of the above issues we must sample initial configuration space efficiently. As noted earlier, MD simulations are not capable of answering the above questions, for such simulations are too compute intensive to allow us to probe the relevant time scales for long chain molecules. We thus now turn to the development of a stochastic model that captures the important physics for the problem at hand, while being computationally tractable. We first describe our coarse grained model for the chain architecture relevant to the PMMA–aluminum system (and the MD simulations), i.e., we consider a chain with two pendant groups per segment that interact strongly with the surface.

IV. TWO STICKER KINETIC ISING MODEL

It is known from MD simulations[11] and experiments[16,17] that the first step of adsorption from solution is fast. The chain molecule is adsorbed initially in some nonequilibrium conformation. The dynamics of the subsequent relaxation of the adsorbed chains is what we wish to probe in the studies to be described here. The events that govern this dynamical behavior are the binding and unbinding of the functional groups on the chain subject to the constraints imposed by the polymer connectivity and the segment–surface interactions.

Once the chain molecule is adsorbed in some arbitrary nonequilibrium conformation, each pendant group that may bind to the surface may be considered to be in either of two states (adsorbed or desorbed). We can label the desorbed and adsorbed states as "spin up" and "spin down," respectively. Furthermore, we can associate the spin up state with a marker $\sigma=+1$ and the spin down state with $\sigma=-1$. Each pendant group is thus mapped onto a spin-1/2 Ising spin, and the vector of $2N$ spin states (where N is the length of the chain) measures the conformation of the adsorbed chain molecule. In other words, we have constructed an isomorphism between adsorbed chain conformation and a spin-1/2 Ising model. The temporal evolution of adsorbed chain conformations can be obtained now by following the dynamics of spin flips. This can be accomplished by solving a master equation with Glauber-type kinetics for the time evolution of the Ising spin states. The dynamical simulation of adsorbed chain relaxation thus consists of following the time evolution of a prepared initial set of spins via the master equation. Average dynamical properties are obtained by averaging over several realizations of the initial prepared state. This averaging is simply an average over initial configuration space, which is necessary since the polymer chains initially adsorb in nonequilibrium conformations.

In order to obtain the time evolution of the spin states via a master equation we need to know the transition probabilities for spin flips to occur. We now turn attention to the formulation of these kinetic expressions for the physical situation under consideration.

For a single independent spin, the transition state theory (TST) kinetic rate expression for desorption would be $k_{\mathrm{des}}=\alpha \exp(-E_{\mathrm{well}}/k_B T)$, where α is the attempt frequency and E_{well} is the adsorption energy. The situation is more complex for a polymer chain, and the adsorption and desorption rates of a given spin depend on the states of the other spins that constitute our model for the adsorbed polymer. We can generalize the rate expressions obtained from TST as follows:

$$k_{\mathrm{des,str}}=\alpha_{\mathrm{str}} f(\text{surrounding spin state}) \times \exp(-E_{\mathrm{str}}/k_B T) \tag{1}$$

and

$$k_{\mathrm{des,\ weak}}=\alpha_{\mathrm{weak}} f(\text{surrounding spin state}) \times \exp(-E_{\mathrm{weak}}/k_B T). \tag{2}$$

The function f embodies the influence of the state of the neighboring spins on the rate of desorption of a given spin. This may be viewed physically as follows. Each spin has a desorption channel available to it corresponding to a rate $\alpha \exp(-E/k_B T)$. The fact that each spin forms a part of a contiguous chain leads to impediments in the desorption channels. The nature of these impediments depends on the states of the spins in the region around the spin under consideration. The function f relates the state of the neighboring region to the nature of the impediments, and their influence on the rate of desorption. Although this point will be discussed in detail later, we note that the dependence of f on the surrounding spin state may lead to highly cooperative relaxation dynamics for the interfacial chains. We do not need to write explicit expressions for the rate of adsorption, because once the desorption rate is specified, the corresponding rate of adsorption is determined by the condition of detailed balance.

We now turn attention to developing the rules that determine the function f. We develop these rules by considering three important physical features that influence the rates of spin flips. First of all, there are steric constraints due to the neighboring chain segments. For example, the rates of desorption and adsorption of a given functional group will be greatly affected by the number of adjacent functional groups that are already adsorbed to the surface. Specifically, contrast a sequence of three monomers adsorbed to the surface with the case wherein only a central segment is bound to the surface; now consider the rate of desorption of this central segment. Clearly, in the former case, the impediments placed on the desorption channels available to a free monomer will be much more severe. Recently Shaffer and Chakraborty have performed stochastic calculations with the full quantum mechanically calculated energy hypersurface of the PMMA–Al system, and find that the rate of adsorption of a given segment is aided when one neighbor is adsorbed and hindered when both neighbors are bound. Effects such as this, we term steric constraints. Shaffer *et al.*[12] have performed quantum

mechanical calculations to map out the energy hypersurface that characterizes the interactions of PMMA oligomers with aluminum surfaces. One interesting result that emerges from these calculations is that sequences of bound segments have several local minima depending on the rotational conformations. Further, many of the local minima correspond to rotational conformations that are strained when compared to the free oligomers. This is simply a result of the fact that favorable interactions between the segments and the surface can stabilize unfavorable rotational conformations in each of the local minima. This implies that a sequence of bound segments is torsionally strained. Experimental evidence for this feature in strongly interacting polymer–solid interfaces also exists. Konstandinidis *et al.*[24] have found via nuclear magnetic resonance (NMR) studies that sequences of bound segments exhibit many more *gauche* conformations than *trans* (compared to the free polymer) upon the nonequilibrium adsorption of PMMA on native oxides of aluminum. This torsional strain must affect the rates of adsorption and desorption, and this is the second physical feature that is incorporated in f. Each spin in our model is part of a contiguous chain molecule. Thus adsorption and desorption events (or spin flips) are associated with changes in configurational entropy. For example, the configurational entropy decreases when an adsorption event causes a loop or a tail of the polymer to shrink. Since the segments of a loop or tail do not explicitly explore the possible loop or tail configurations, these entropy changes must be incorporated into the transition probabilities. This is the third physical effect that must be incorporated in f. We now develop mathematical rules that account for the three effects outlined above.

The steric constraints are derived by close examination of the results of molecular dynamics simulations of short polymer chains. In order to see the effects of steric constraints imposed by adjacent segments, two scenarios can be envisaged. Consider first a central chain segment with both pendant groups adsorbed. If both functional groups on one of the two neighboring segments are desorbed, then sufficient configurational flexibility is present for a central segment functional group to desorb. Now consider the situation wherein only one of the two pendant groups on a central segment is adsorbed. In this case, the spin can desorb unhindered only if at least one pendant group is desorbed on the left or right segments. If not, desorption events are hindered.

These steric constraints to desorption can be put in mathematical form by defining the following facilitation functions. For the first circumstance, we define the facilitation function β to be

$$\beta=[q(q-1)+r(r-1)]/4, \tag{3}$$

where q and r are the number of up spins on the left and right segments, respectively, and β is nonzero if two spins are up on at least one neighboring segment. Equation (4) represents a two-spin facilitation function.

In the second circumstance we employ a one-spin facilitation function

$$\beta=(q+r)/4, \tag{4}$$

where β is nonzero if at least one spin is up on a neighboring segment. The factors of 4 in the denominators normalize the facilitation functions to range from zero to unity. In highly adsorbed configurations, it is rare for both the left and the right stickers to be desorbed. Thus β is rarely unity. The steric constraint function β forbids certain local spin flips in highly adsorbed chain configurations. We note that similar constraint functions have been employed[25–28] to model bulk glass-forming liquids.

The presence of rotationally strained sequences of bound segments in a chemisorbed chain arises from the strong and specific segment–surface interactions. A torsion angle that corresponds to a high energy state for the free polymer may be induced as a functional group binds to the surface. In highly adsorbed configurations this strain is difficult to relax. For example, if both pendant groups on a segment are adsorbed, this freezes the rotational motion of that segment. Consequently, an adjacent segment may be forced to adopt a rotationally strained configuration when adsorbing or desorbing. Consider a particular segment of the chain with both pendant groups adsorbed. If both pendant groups on an adjacent segment are adsorbed then the polymer backbone is locally *trans*, and there is no rotational strain between the two segments. If both pendant groups on the adjacent segment are desorbed then the adjacent segment is rotationally mobile and there is no rotational strain between the two segments. However, if exactly one group on the adjacent segment is adsorbed, then there must be rotational strain between the two segments. Rates of events that relieve rotational strain must be enhanced. In our model, we account for this by discretizing the rotational states as indicated above. If a strained state exists, the rates of spin flips that relax rotational strain are enhanced by the Boltzmann factor $\gamma=\exp(E_{\text{tor}}/k_BT)$. In all unstrained configurations $\gamma=1$. Note that when determining γ we examine the state of both neighboring segments with pendant groups. We take E_{tor} as the barrier height of the threefold symmetric modification of the torsion potential for butane (3.5 kcal/mol).

As noted earlier, the configurational entropy of a chain molecule changes when adsorption and desorption events lead to changes in the distribution of loops, trains, and tails. The change in entropy associated with a given event can be obtained from the following expressions for the loop and tail entropies [S_{loop} and S_{tail} (Ref. 29)]:

$$S_{\text{loop}}=k_B[(L-1)\ln z-\tfrac{3}{2}\ln L] \tag{5}$$

and

$$S_{\text{tail}}=k_B[(L-1)\ln z-\tfrac{1}{2}\ln L], \tag{6}$$

where L is the length of the loop or tail, and z is the coordination number of the lattice. These entropy expressions arise from considering ideal random walks on a lattice and are therefore a simple, leading order treatment of the changes in chain entropy associated with adsorption and desorption events. We employ a simple cubic lattice with $z=6$ for the present calculations. The entropy penalty

to the transition probability for adsorption is $\delta=\exp(\Delta S/k_B)$, where ΔS is the change in entropy upon adsorption and is negative, thus hindering the adsorption rate. For desorption events $\delta=1$, thus the ratio of adsorption and desorption rates yields the correct equilibrium entropy change. Note that the length scales that determine δ are the loop and tail sizes, which can be much longer than those that determine the steric and rotational constraints. In the initial stages of strong adsorption and at all times for weak adsorption, the loop and tail sizes tend to be large. In other words, the rate of an individual spin flip can be correlated to the state of neighboring spins over long length scales.

Combining the steric constraints, rotational strain, and entropic changes as $f(\text{surrounding spin state})=\beta\gamma\delta$ specifies the overall facilitation function.

Returning now to the attempt frequencies α_{str} and α_{weak}, the simplest expression for the attempt frequency is that obtained from TST. For a single atom in a parabolic energy well, the oscillation frequency about the potential energy minimum is

$$\alpha=(1/2\pi)\sqrt{\kappa/m}, \tag{7}$$

where κ is the curvature at the minimum of the energy well and m is the mass of the atom. Specifying the attempt frequency is equivalent to specifying the intrinsic physical time scale for the events under consideration. We specify α by establishing the connection between the time scales of the MD simulation (which explicitly includes the solvent and the polymer bond bending and torsion) and the kinetic Ising model.

Substitution of m and κ values for the potentials employed in the MD simulation yield $\alpha_{\text{str}}=10.1\ \text{ps}^{-1}$ and $\alpha_{\text{weak}}=7.14\ \text{ps}^{-1}$. These values should not be directly employed in simulations using the kinetic Ising model if we wish to obtain the correct time scales for the dynamical phenomena under consideration. This is so because the coarse graining involved in constructing the kinetic Ising model and ignoring the presence of solvent will influence the time scale sampled by the model. Thus, we obtain the intrinsic time scales for the kinetic Ising model by comparing the results of such calculations with full MD simulations for short chains. Such comparisons serve another important purpose. As we have seen, the rules that determine f have been obtained by physical induction rather than rigorous deduction. As such, prior to using our model to study adsorbed chain relaxation over time scales inaccessible to MD we must validate our model by comparison with MD simulations for short chains. Once this comparison enables us to validate our model for the stochastic dynamics and establish the correct intrinsic time scale for the kinetic Ising model we can turn to the simulation of long chains over long time scales.

MD simulations were performed for short times for octamers of our model chain over a range of temperatures (or E_{weak}/k_BT). Calculations using the Ising model were also performed over the same range of temperatures for octamers. Details of how these calculations are performed will be provided presently; herein we simply state that the dynamical behavior is obtained by numerically solving the master equation using the Monte Carlo method.

At $E_{\text{weak}}/k_BT=1.92$, the average desorption time per sticker obtained from the MD simulations was 21 and 7 ps for the strong and weak stickers, respectively. Under similar conditions, the Ising model calculations (using $\alpha_{\text{str}}=10.1\ \text{ps}^{-1}$ and $\alpha_{\text{weak}}=7.14\ \text{ps}^{-1}$) yielded average desorption times of 124 and 36 ps for the strong and weak stickers, respectively. The ratio of average desorption time is thus 5.9 and 5.1 for the strong and weak stickers, respectively. To set the time scale for our model, the attempt frequencies for the Ising model are increased by a factor of 6. Clearly, the time scale conversion is crude. However, we consider it sufficient for the study of the qualitative features of the dynamical behavior of strongly adsorbed polymer chains. As an alternative to adjusting the attempt frequencies, we may view the factors of 5.9 and 5.1 as being associated with the facilitation function, f. This view has the merit of retaining the physical significance of the attempt frequencies. However, with respect to studies of the dynamical behavior of adsorbed chains, the two points of view are indistinguishable. We note that upon using the new values of α, the results of the kinetic Ising model for octamers match those obtained from the MD simulations over a range of temperatures ($E_{\text{weak}}/k_BT=1$–8.5) both in terms of final states and the average dynamical behavior observed on a coarse-grained time scale.

Having established the time scale and validated our model, we may now proceed to study the dynamical behavior of long chains over a range of segment–surface interaction energies using our stochastic model. Since the stochastic model is four orders of magnitude less compute intensive compared to MD simulations, we can simulate long chains and average over several realizations of the initial adsorbed configuration. Such averaging over initial configuration space is necessary in order to study the nonequilibrium phenomena under consideration. The results reported in this paper represent an averaging over at least five realizations of the initial adsorbed state.

The Ising simulations are initialized by randomly adsorbing 10% of the segments. We find that the simulation results are not sensitive to variations in the initial adsorbed fraction since many pendant groups adsorb in the first few time steps, washing away the memory of which groups were initially adsorbed.

We employ 2 fs time steps, where the probability of the most favorable adsorption or desorption event is still small (on the order of 2%). Multiple adsorption and desorption events may occur on the same time step, but this almost always occurs in locations on the chain that are well separated, and so the events are essentially independent and no decision need be made about which event occurred first. Under highly adsorbed conditions there are few stickers which can change state. The result is that nothing happens for many time steps. This inefficiency is mitigated by the fact that the computationally expensive transition probabilities do not need to be recalculated after time steps with zero events. A possible alternative methodology,[30] which we do not employ, is to step in time from event to event. In

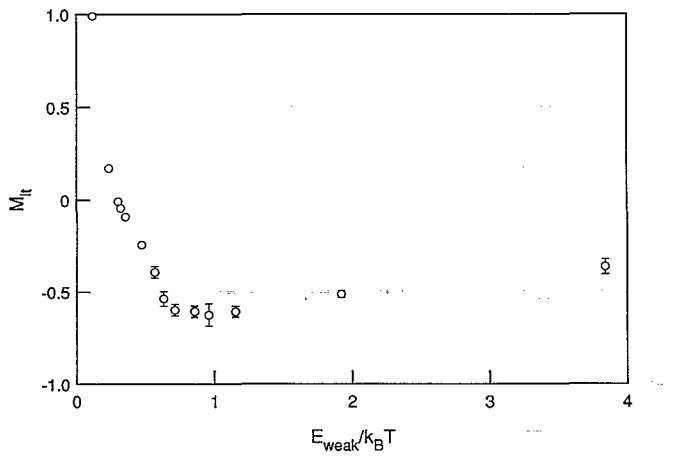

FIG. 1. Long time average of weak sticker adsorption, M_{lt}, for a chain of 500 segments as a function of adsorption energy normalized by the thermal energy k_BT. $M_{lt}=\langle\sigma\rangle$, where σ is $+1$ and -1 for desorbed and adsorbed stickers, respectively. Equilibrium adsorption for high temperatures, nonequilibrium for low temperatures.

this method the time step is irregular and exactly one event occurs with each time step. We choose the equal time step method for its simpler algorithm, ease of generating time correlation functions, and ease of comparison to the equal time steps of the MD simulation. We note that for more complicated situations, such as atomistic dynamical simulation of polymers interacting with chemisorbing surfaces, such an alternative method is highly efficient and should be employed.[23]

V. RESULTS AND DISCUSSION FOR TWO STICKER ISING MODEL

The temporal evolution of the chain conformations can be monitored by the change in the number of adsorbed pendant groups. At long times the number of adsorbed stickers must equilibrate, but as noted in previous papers,[11,14] for strongly adsorbed chains this may not be possible in realistic time scales.

At high temperatures, few pendant groups are adsorbed and equilibration is rapid. The low and intermediate temperature regimes, which correspond to strong and intermediate segment–surface interaction energies, will be our focus in what follows. A measure of the number of sorbed pendant groups is the average magnetization, defined as $M=\langle\sigma\rangle$; the average being defined over all spins. We turn attention first to the long time value of M as a function of temperature (or segment–surface interaction energies). Figure 1 shows our results for the long time average of the magnetization, denoted by M_{lt}. These results are for a polymer chain of 500 segments.

At high temperatures (small E_{weak}/k_BT) the polymer chain is weakly adsorbed and is equilibrated. The degree of adsorption varies rapidly with temperature from nonadsorbing, $M_{lt}=1.0$, to highly adsorbed. At low temperatures the degree of adsorption corresponds to a nonequilibrium *situation* since M_{lt} has a minimum and then increases as temperature goes to zero (large E_{weak}/k_BT), contrary to equilibrium adsorption behavior which goes to $M_{lt}=-1.0$ as temperature goes to zero. This departure from equilibrium represents a dynamical falling out of equilibrium for the adsorbed chains. Such a surface induced vitrification of the adsorbed polymer chains has been considered by us heretofore;[11,14] the results of Fig. 1 demonstrate this physical phenomenon unequivocally. As noted earlier, the existence of these nonequilibrium structures motivates the study of the dynamical behavior of strongly adsorbed polymer chains. Specifically, we wish to study the kinetics of adsorbed chain relaxation as the conformations evolve toward equilibrium.

The relaxation to equilibrium can be conveniently measured by

$$\psi(t)=\frac{M(t)-M_{eq}}{1-M_{eq}}, \tag{8}$$

where M_{eq} is the equilibrium value of M at a given temperature.

The temporal evolution of adsorbed chain structure proceeds slowly at low temperatures. At $E_{weak}/k_BT=3.84$ and $E_{str}/k_BT=7.68$, the polymer is frozen on the time scale of the simulation (150 ns), as is shown in Fig. 2(a), note that equilibrium corresponds to $\psi(t)=0$. In fact, at this temperature the polymer should remain trapped in nonequilibrium states even over experimental time scales. We emphasize that this trapping is due to strong and specific interactions with the surface. It is a separate phenomenon from any glass transition that the polymer may undergo as a bulk material.

At low temperatures (or high segment–surface interaction energies), after the initial fast adsorption, the chains are trapped in nonequilibrium states because sequences of bound segments are trapped in deep local minima ($\gg k_BT$); kinetic constraints do not allow the chain structure to evolve such that is acquires its global minimum of free energy in any realistic time scale. In other words, the physical system has effectively broken ergodicity.

At a higher temperature, escapes from local minima become more probable and we can observe the slow relaxation of the chain on the simulation time scale. In Figs. 2(b), 2(c), and 2(d) we see the chain relaxation for $E_{weak}/k_BT=0.96$, 0.72, and 0.576, respectively. For this range of temperatures, relaxation to equilibrium does occur. However, we find that the kinetics of relaxation cannot be described by the Debye form with one relaxation time. As shown in Fig. 2, the kinetics of relaxation are best described by a *KWW* expression or stretched exponentials, i.e.,

$$\psi(t)=\exp[-(t/\tau)^{\beta}]. \tag{9}$$

Note that we find the stretching parameter, β, to be significantly different from unity and to be temperature dependent. The fact that the kinetics of adsorbed chain relaxation is best described by stretched exponential functions shows that the dynamical behavior is not simple and is akin to that observed for bulk glass-forming liquids. This point deserves detailed discussion.

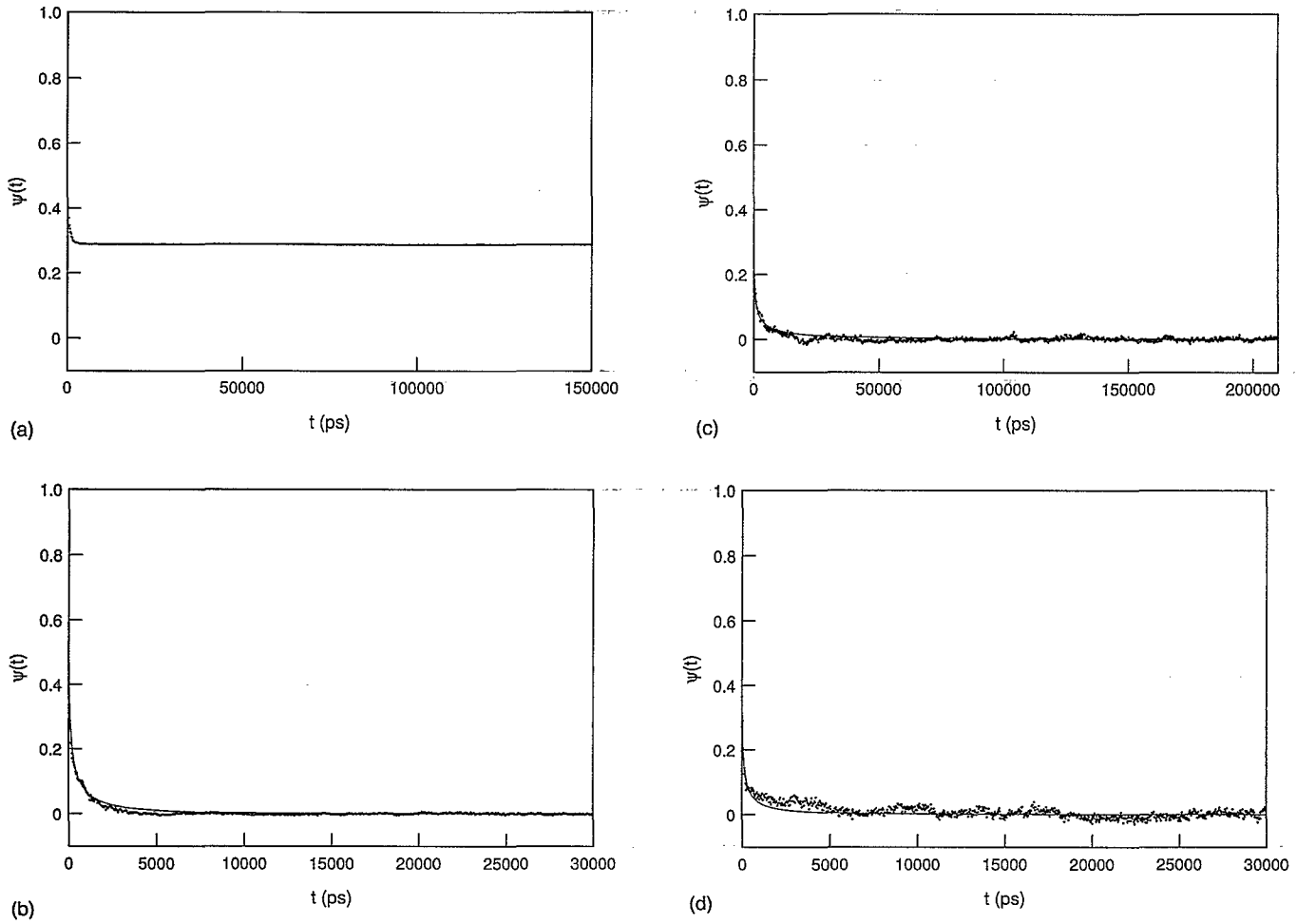

FIG. 2. Weak sticker relaxation for 500 segment chain $\psi(t)=[M(t)-M_{eq}]/(1-M_{eq})$ as a function of time for (a) $E_{weak}/k_BT=3.84$ and $M_{eq}=-0.99$; (b) $E_{weak}/k_BT=0.96$ and $M_{eq}=-0.63$; (c) $E_{weak}/k_BT=0.72$ and $M_{eq}=-0.60$; and (d) $E_{weak}/k_BT=0.576$ and $M_{eq}=-0.39$. (—) is *KWW* fit of $\psi(t)$.

Ever since Kohlrausch[31] it has been known that the dynamical behavior of many complex fluids do not follow the simple Debye form. Since that time, several dynamical quantities for glass-forming liquids have been found to obey the *KWW* expression.[32] Theoretical efforts[22,25–28,32] aimed toward understanding this behavior for bulk liquids have shown that as the temperature at which the system dynamically falls out of equilibrium is approached from above, the dynamics become highly cooperative. One theoretical study due to Palmer *et al.*[22] is particularly useful in understanding this physical phenomenon. In this work, these authors show that a general class of dynamical models (which they term hierarchically constrained) would lead to stretched exponential relaxation functions. The physical content of the class of hierarchically constrained models is the following. In any complex physical system there are many degrees of freedom. Consider the situation wherein the degrees of freedom are not all equivalent, but rather form a hierarchy of levels. A hierarchically constrained dynamical model is one wherein the relaxation of a higher level degree of freedom requires that degrees of freedom at lower levels be in certain prescribed states. This leads to highly cooperative dynamical behavior, and Palmer *et al.*[22] have shown that stretched exponential relaxation functions result for specific choices of the nature of the prescribed states.

The degrees of freedom in our system may be considered to be the state of each of the pendant groups in our model polymer. In a real polymer–solid interface (e.g., PMMA–aluminum system) there are a greater number of degrees of freedom per monomer (orientation and distance from the surface, and internal configurational degrees of freedom).[12] As has been shown before,[12] the energy hypersurface exhibits several deep local minima in the space of these degrees of freedom. This is due to the fact that the binding energy of a given functional group depends upon its orientation with respect to the surface and the configuration of the rest of the chain. This "rugged" energy landscape[33] is the reason for the probability of a functional group making a transition to be strongly dependent on the location of other parts of the chain in configuration space. This is the origin of the cooperative dynamical behavior of our system, and may be viewed in terms of the model due to Palmer *et al.*[22] Consider an individual spin (pendant group) in our model. Let us say that we wish to find the probability of this spin flipping. We define the state of this spin to be the highest level degree of freedom since it is the focus of our attention. The states of all the other spins that

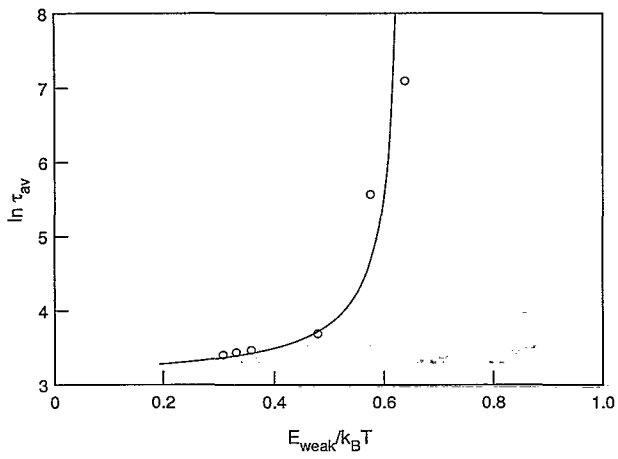

FIG. 3. Arrhenius plot of average relaxation time τ_{av} for 500 segment chain showing non-Arrhenius behavior fit by the Vogel–Fulcher law. Diverging relaxation time is a signature of glassy dynamics and glass transition temperature.

constitute the adsorbed chain are lower level degrees of freedom. For the highest level degree of freedom to relax (i.e., for the spin to flip), our model requires that the lower level degrees of freedom (the other spins) be in certain prescribed states. Put another way, the function f is such that, spin flips cannot occur if the other spins constituting the chain molecule are in certain states. Thus our model for the physical situation of strongly adsorbed chains may perhaps be viewed as being in the same dynamical universality class as the hierarchically constrained models of Palmer *et al.*. The origins of stretched exponential relaxation kinetics for our system may be viewed in yet another way. Non-Debye relaxation can occur if a system possesses a highly dense spectrum of relaxation times or activation energies. In our model, the rate of spin flips for a given spin is highly dependent on the state of its neighbors. Each spin has a different environment, which leads to different effective rates. Thus, we have a host of relaxation times and activation energies characterizing adsorbed chain relaxation.

Further evidence of adsorbed polymer chains behaving like glassy materials with highly cooperative dynamics over a range of temperatures is provided in Fig. 3. Herein, we have plotted the average relaxation time for the adsorbed polymer chain as a function of temperature. The average relaxation time τ_{av} is defined such that it is independent of the form of the relaxation function $\psi(t)$ used to fit the kinetics associated with the number of sorbed segments relaxing to equilibrium. We define an average nonlinear relaxation time to be the area under the curve, $\psi(t)$ vs t. In Fig. 3, τ_{av} is plotted as a function of temperature in the form suggested by Arrhenius.[34] As we can see, the calculated points show that the behavior is highly non-Arrhenius. In fact, the data can be fit by the Vogel–Fulcher (VF) (Refs. 35–37) law, $\tau_{av}=\tau_0 \exp[-E_a/k_B(T-T_0)]$. We do not attach great significance to the fact that the VF equation fits the data, except in that there is a divergence of the relaxation time at finite temperature. This is akin to the behavior of many bulk glass-forming liquids, and the parameter T_0 in the VF equation may be interpreted to be the temperature below which there is a dynamical falling out of equilibrium. For the case at hand, this surface induced vitrification temperature appears to be $1.54E_{weak}/k_B$.

We note (as shown in Fig. 4) that other dynamical quantities, such as the one-spin time correlation function, also follow stretched exponential relaxation over a range of temperatures.

The recent experimental work of Granick and coworkers[16,17] has provided insight into the dynamics of strongly adsorbed chains. Their system consists of initially adsorbed polystyrene (PS), $E_{ads}/k_BT \approx 1.3$ and then adsorption of PMMA, $E_{ads}/k_BT \approx 4$. Johnston and Granick have employed infrared spectroscopy to measure the number of sorbed PMMA segments as a function of time. These authors have plotted their experimental data in the form of our binding fraction ψ as a function of time and extracted an average relaxation time from this data. Their experiments have found stretched exponential relaxation kinetics with β near 0.5 and τ_{av} on the order of hours or days. Furthermore, the temperature dependence of the average relaxation time is non-Arrhenius, with the relaxation times fit well by the VF law, and thus showing an apparent divergence in the relaxation time at a finite temperature. Both of these results are consistent with our model predictions. The value of $\beta=0.5$ is within the range of β from our simulations. The experimental time scale is much longer than the time scales accessible via simulation, but we can see that the experimental adsorption energies are above the point where the VF law (Fig. 3) predicts divergence in the relaxation time scale. Furthermore, the experimental conditions consist of an entire layer of adsorbed polymer rather than the low coverage limit of isolated chains. We believe (as Ref. 16 suggests) that interchain interactions, namely the steric constraints imposed on each chain by the other chains provide further impediments to adsorption–desorption events. These interchain effects are enhancements of the steric constraints present in our model, and should lead to a richer energy landscape than that considered in this paper. The qualitative behavior should be (and is) the same.

VI. ONE STICKER KINETIC ISING MODEL

The two sticker model that we have developed and described in the previous section corresponds to a particular polymer architecture, one wherein there are two functional groups per segment that can chemisorb to a surface. This architecture is appropriate for such polymers as PMMA with its carbonyl and methoxy functional groups, both of which chemisorb to an aluminum surface. Other polymer architectures should be described by generalized versions of our kinetic Ising model. The polymer architecture consisting of one chemisorbing functional group per segment is of interest due to its inherent simplicity. The development of a one sticker kinetic Ising model is presented below, and then followed by the simulation results from this model. Our main interest is to determine the effect of chain architecture on the dynamical behavior.

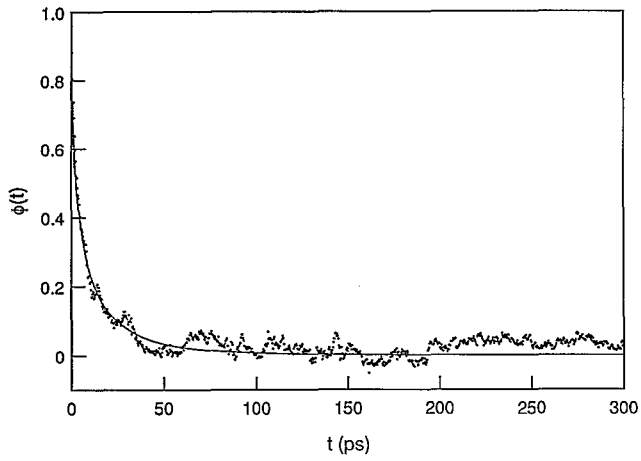

FIG. 4. Weak sticker one-spin time correlation function $\phi(t)$ for 500 segment chain for $E_{\text{weak}}/k_BT=0.96$ and KWW fit parameters $\beta=0.53$ and $\tau=5.07$ ps.

Therefore our focus is to compare and contrast the dynamical results of the one sticker and two sticker architectures.

The one sticker kinetic Ising model is different in detail from the two sticker model. In the one sticker architecture, each functional group along the polymer chain is identical and has the same adsorption energy. In contrast, two energy scales of strong and weak adsorption groups are present in the two sticker architecture. The steric constraint, i.e., the reduced mobility of a functional group when neighboring functional groups are already adsorbed to the surface, is similar in the one and two sticker architectures. However, the one sticker architecture has two nearest neighbors whereas the two sticker geometry has five nearest neighbors. The consequences of this reduced number of nearest neighbors will be discussed in greater detail below. Rotational strain effects should not be significant in the one sticker architecture. With only one adsorption group per segment, the backbone torsion angles of the chain are not forced into strained positions to accommodate the adsorption. Thus, no torsional energy penalty is associated with any adsorbed configuration. Finally, the entropic penalties incurred in polymer adsorption are the same for the one sticker and two sticker architectures. The configurational entropy decreases when an adsorption event causes a loop or a tail of the polymer to shrink. Although the entropy changes in the two different architectures are calculated in exactly the same way [via Eqs. (6) and (7)], the entropic effects are more important in the one sticker model. Each spin flip in the one sticker model must change a loop or tail size, whereas in the two sticker model a spin flip may leave the loop and tail sizes unchanged. Thus, the one sticker architecture has entropic changes for every adsorption or desorption event.

We now develop kinetic expressions for the one sticker architecture. We begin with the general rate expression given by Eq. (2), but we drop the distinction between strong and weak stickers, yielding

$$k=\alpha f(\text{surrounding spin state})\exp(-E/k_BT), \qquad (10)$$

where we take the attempt frequency as $\alpha=24.0\ \text{ps}^{-1}$ and the adsorption energy as $E=7.5\epsilon_{\text{LJ}}$.

As the first component of f, the steric constraints are taken to be similar to the two sticker model. We consider the nearest neighbors and the next nearest neighbors of a given segment, i.e., the two spins on the left and the two spins on the right. We define a two-spin facilitation function as

$$\beta=[q(q-1)+r(r-1)]/4, \qquad (11)$$

where q and r are the number of up spins on the left and right, respectively, and β is nonzero if two spins are up on at least one side. Note that for the two-sticker model, the steric constraints were incorporated by a mixture of two-spin and one-spin facilitation functions. We postulate that no rotational strain exists in the adsorbed one sticker chain configuration, so $\gamma=1$ for all configurations. The entropic effect of adsorption is $\delta=\exp(\Delta S/k_B)$, where ΔS is calculated from Eqs. (6) and (7) just as in the two sticker architecture. Combining the three contributions yields $f=\beta\gamma\delta$ just as before.

Let us turn now to the simulation results for the one sticker architecture. The temperature dependence of the long time degree of adsorption, M_{lt}, is shown in Fig. 5(a) (for chains of length 1000). At high temperatures (small E/k_BT), few pendant groups are adsorbed and equilibration is rapid, while at lower temperatures there are many adsorbed pendant groups and slower dynamics. An important advantage in the simulation of the one sticker architecture is the existence of analytical equilibrium predictions for the degree of adsorption as a function of adsorption energy (or temperature). In Fig. 5(a) the simulation results are compared to statistical mechanical equilibrium predictions by Hoeve *et al.*.[38,39] Note that the equilibrium calculations are for an infinite chain without kinetic constraints. Hoeve *et al.* develop their results in terms of the ratio of adsorbed and desorbed segment level internal partition functions and in terms of a chain stiffness parameter. Thus to apply their results these parameters must be determined for our model polymer. The adsorption energy, E/k_BT, and the simple entropy equations (with lattice coordination number z) suffice to determine the Hoeve parameters. We must take the Hoeve stiffness parameter to be $1/z$ and the Hoeve ratio of adsorbed and desorbed partition functions to be $(1/z)\exp(E/k_BT)$ in order to describe the polymer chain employed in the simulations.

The analytical equilibrium results and the kinetic Ising model simulation results are shown in Fig. 5(a) as the solid line and the data points, respectively. The analytical equilibrium results agree well with the simulation results at high temperatures (under conditions of weak adsorption) as expected since equilibration should be rapid under weak adsorbing conditions. At intermediate temperatures the simulation results are more strongly adsorbing than the equilibrium predictions. This effect is due to the kinetic constraints, a train of adsorbed segments is hindered from

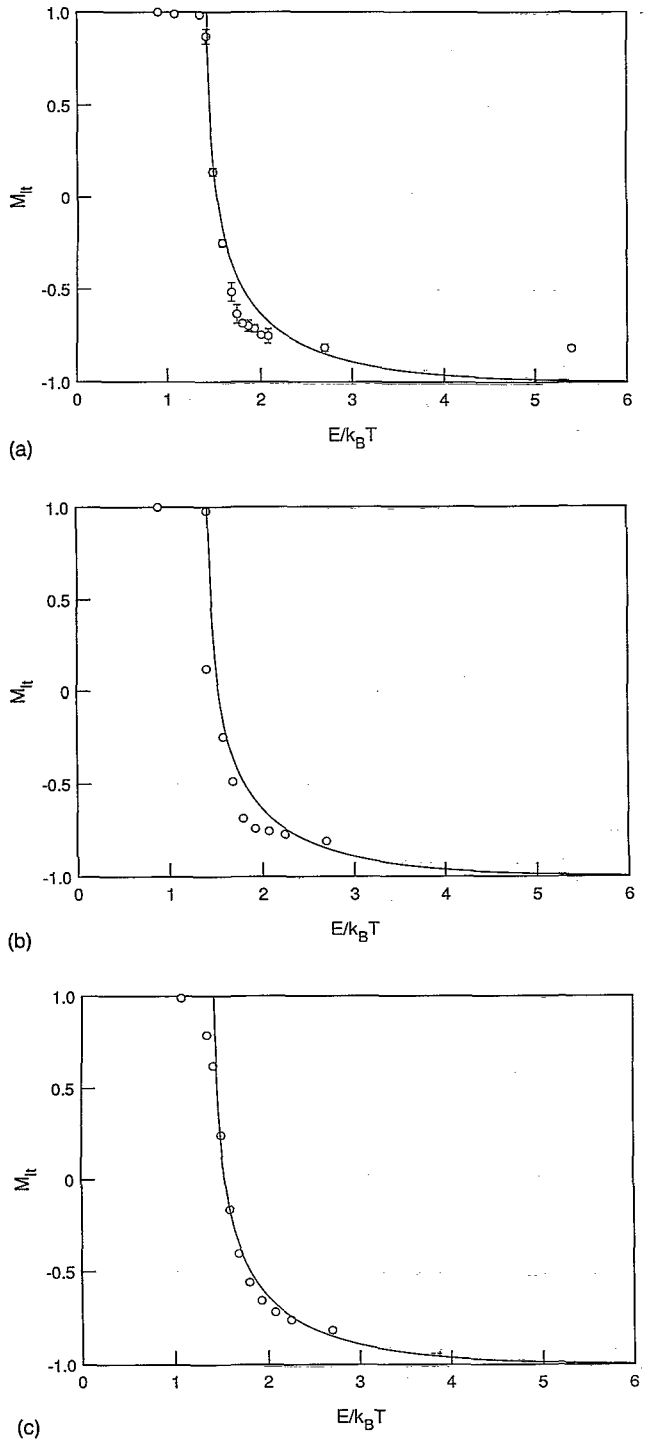

FIG. 5. Long time average of sticker adsorption, M_{lt}, for a chain of (a) 1000; (b) 10 000; and (c) 100 segments as a function of temperature T. $M_{lt}=\langle\sigma\rangle$, where σ is $+1$ and -1 for desorbed and adsorbed stickers, respectively. Equilibrium adsorption for high temperatures, nonequilibrium for low temperatures. (—) is equilibrium theory for infinite chain and no kinetic barriers.

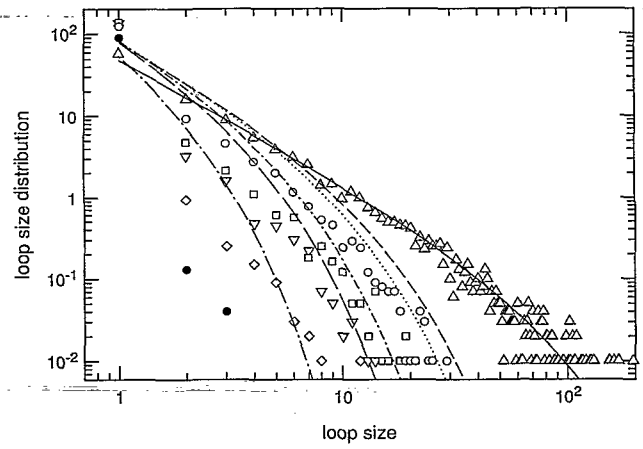

FIG. 6. Temperature dependence of the loop size distribution for a 1000 segment chain. Simulation results with kinetic constraints for E/k_BT $=1.5$, 1.69, 1.74, 1.93, 2.08, 2.7 (△, ○, □, ▽, ◇, ●, respectively). Equilibrium theory for infinite chain and no kinetic barriers, at the same E/k_BT as above (—, ---, ···, -·-, - - -, —·—·—, respectively).

desorption and the average degree of adsorption is greater. At low temperatures the simulation is frozen in nonequilibrium states that are less adsorbed than equilibrium. As expected, the equilibrium shifts to complete adsorption as temperature goes to zero. Thus at low temperatures (or large segment–surface interactions) the polymer is far from equilibrium. We see that the qualitative temperature dependence of the long time degree of adsorption is similar for the one sticker and two sticker architectures, where both have a dynamical falling out of equilibrium at low temperatures.

The chain length dependence of the degree of adsorption is of interest, especially to determine what length is sufficient to have chain adsorption that is representative of the long chain limit. Figure 5(b) shows that the degree of adsorption of a 10 000 segment chain is the same as that for the 1000 segment chain of Fig. 5(a). This shows that we are already in the long chain limit with 1000 segments. On the other hand, Fig. 5(c) shows that the degree of adsorption of 100 segment chains differs from the 1000 segment chains. At intermediate temperatures the 100 segment chains are significantly less adsorbed than the 1000 segment chains, hence a chain of length 100 is too short to yield the adsorption dynamics of the long chain limit.

The loop size distribution provides a detailed picture of the adsorbed chain configurations. The loop size distribution is shown in Fig. 6 for six different temperatures in the range $E/k_BT=1.5$–2.7. The loop size distribution is obtained from a time average over the second half of each simulation, wherein the chain configurations have relaxed to their long time behavior. One hundred chain configurations were saved during the second half of each simulation and were averaged together to yield the loop size distribution. For comparison, the analytical results of Hoeve *et al.*[38,39] for the equilibrium loop distribution (without kinetic constraints) are shown in Fig. 6 for the same temperatures as in the simulations. The analytical and simulation results are in excellent agreement over the whole range of loop sizes for the highest temperature results (E/k_BT $=1.5$). At this temperature, the loop distribution shows a wide range of loop sizes, wherein the largest loop size is on the order of 100 segments. At lower temperatures, the loop

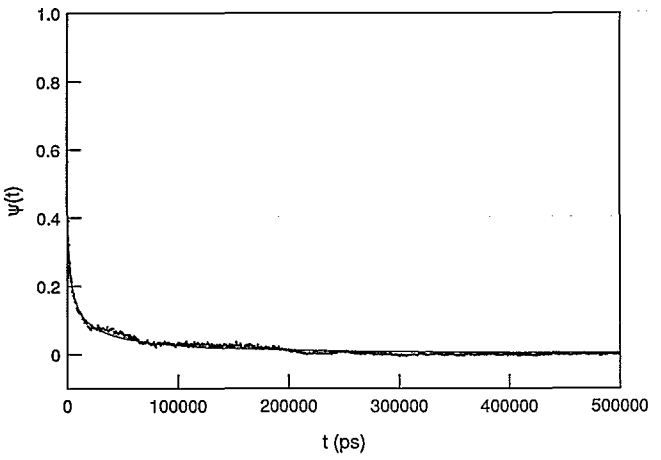

FIG. 7. Sticker relaxation for 1000 segment chain $\psi(t)=[M(t)-M_{eq}]/(1-M_{eq})$ as a function of time for $E/k_BT=2.0$ and $M_{eq}=-0.75$. (—) is *KWW* fit with $\beta=0.26$ and $\tau=680$ ps.

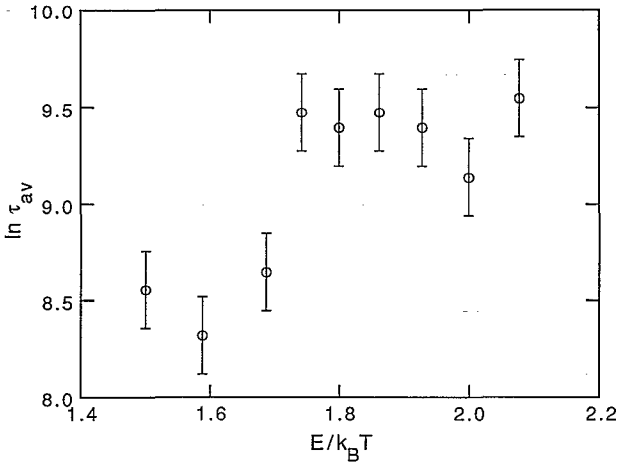

FIG. 8. Arrhenius plot of average relaxation time τ_{av} for 1000 segment chain showing non-Arrhenius behavior. Two regimes of relaxation time at high and intermediate temperatures.

size distribution shifts toward fewer and smaller loops and a high degree of adsorption. The simulation and equilibrium results show an increasing deviation from one another as the temperature drops. The simulation results show fewer and smaller loops than the analytical equilibrium results. At low temperatures and high degrees of adsorption, the kinetic constraints incorporated into the simulation become increasingly important. In contrast, the analytical results are for chain adsorption without kinetic constraints. The shift toward smaller and fewer loops in the simulation results is consistent with the enhanced degree of adsorption seen previously in Fig. 5(a). The kinetic constraints have the effect of hindering the desorption of adsorbed segment trains and increasing the average degree of adsorption.

The time evolution of the degree of adsorption for the one sticker model is similar to the two sticker model. As in the two sticker architecture, we measure the approach to equilibrium with the relaxation function $\psi(t)$ defined in Eq. (9). In Figure 7 the relaxation function $\psi(t)$ is shown for a chain length of 1000 segments for $E/k_BT=2.0$. The relaxation function is fit with the *KWW* law [Eq. (10)] employing $\beta=0.26$, which suggests considerable cooperativity. The fact that both architectures show stretched exponential relaxation kinetics is consistent with the idea that stretched exponential relaxation is a general characteristic of strongly adsorbing polymer chains.

As before, we define an average relaxation time to be the area under the curve, $\psi(t)$ vs t. The temperature dependence of the average relaxation time τ_{av} is strikingly different for the one sticker and two sticker models. An Arrhenius plot of average relaxation time for the one sticker model (Fig. 8) shows two relaxation time scales at high and intermediate temperatures that differ by only a factor of 2. Of course, as seen in Fig. 5(a), at the lowest temperature the chains are trapped in nonequilibrium conformations that do not relax to equilibrium in experimental time scales; i.e., ergodicity is effectively broken and the relaxation time diverges. This result is in striking contrast to the results of the two sticker model where the relaxation time scale diverges according to the VF law. The temperature dependence of the one sticker relaxation time suggests weaker cooperativity for the one sticker architecture and shows that the temperature dependence of τ_{av} is sensitive to the details of the adsorbing chain architecture. While it is clear that the relaxation dynamics for the one sticker architecture is less constrained, we cannot make a detailed connection between the reduced cooperativity and the unusual temperature dependence of the average relaxation times.

The comparison of the dynamical behavior of the one sticker and two sticker chain architectures shows that stretched exponential relaxation is a common feature. In contrast, the temperature dependence of the average relaxation times differ considerably. For the two sticker architecture, the average relaxation time is strongly non-Arrhenius and diverges according to the VF law. The temperature dependence of the average relaxation times for the one sticker architecture, however, are unusual (as discussed above). Further stochastic simulation studies with real polymers[23] may help shed light on this issue.

VII. CONCLUSION

In summary, we consider the relaxation dynamics of a polymer chain that chemisorbs to a solid surface. The strong and specific interactions of the chemisorptive functional groups give rise to energy hypersurfaces with many deep energy minima separated by high transition barriers between states. Consequently, adsorbed chains are trapped in local energy minima and there are slow transitions between conformational states of the adsorbed chain. Thus, relaxation to equilibrium is slow and trapped, nonequilibrium conformations relax with highly cooperative dynamics. We must follow the chain dynamics explicitly to determine the nonequilibrium states, but molecular dynamics simulations are far too compute intensive to examine dy-

namics over long time scales. Therefore, a stochastic model is required. We have developed a spin-1/2 kinetic Ising model for the chain dynamics where the spin flips correspond to the adsorption and desorption events of chemisorptive functional groups. We employ this kinetic Ising model to examine the relaxation dynamics of the two sticker and one sticker chain architectures. The simulation results for the relaxation dynamics of strongly adsorbed chains show that relaxation to equilibrium is an extremely slow and cooperative process under conditions of strong adsorption. At low temperatures the adsorbed chains are trapped in nonequilibrium conformations, and ergodicity is effectively broken. At higher temperatures, the cooperative dynamics give rise to stretched exponential relaxation characteristic of glassy materials.

The temperature dependence of chain relaxation dynamics is sensitive to the polymer architecture. For the two sticker architecture, the average relaxation time diverges according to the VF law. In contrast, the one sticker architecture exhibits a temperature dependence for the average relaxation time that does not obey the VF law.

The experimental work of Granick and co-workers[16,17] for strongly adsorbed PMMA shows both stretched exponential relaxation and VF temperature dependence for the average relaxation time. Both of their results agree well with simulation results of the two sticker architecture (which corresponds to the chemisorbing carbonyl and methoxy functional groups of PMMA). Note that their time scales for relaxation are longer than our predictions. This difference is due to the additional steric constraints arising from interchain interactions. Additional steric constraints increase the chain relaxation cooperativity and slow the chain relaxation time.

The glasslike behavior exhibited by the unique confined fluids under investigation present many unresolved issues. Addressing these might lead to insights not only into the technologically relevant issue of adhesion, but also into the behavior of more complex materials that break ergodicity. These issues are currently being addressed in our laboratories via more sophisticated stochastic dynamical models,[23] and NMR spectroscopy.

ACKNOWLEDGMENTS

Partial financial support for this work was provided by the Director, Office of Basic Energy Sciences, U.S. DOE, under Contract No. DE-AC03-76SF0098, Shell Foundation, and the Dexter Corporation.

[1] R. J. Roe, J. Chem. Phys. **43**, 1591 (1965); **44**, 4264 (1966).
[2] J. M. H. M. Scheutjens and G. J. Fleer, J. Phys. Chem. **83**, 1619 (1979); **84**, 178 (1980).
[3] P. G. de Gennes, *Scaling Concepts in Polymer Physics* (Cornell University, Ithaca, 1979).
[4] I. S. Jones and P. J. Richmond, J. Chem. Soc. Faraday Trans. II **73**, 1062 (1977).
[5] H. J. Ploehn and W. B. Russel, Macromolecules **22**, 266 (1989).
[6] K. F. Freed, *Renormalization Group Theory of Macromolecules* (Wiley, New York, 1987).
[7] A. Takahashi and M. Kawaguchi, Adv. Polym. Sci. **46**, 1 (1982).
[8] H. Leidheiser Jr. and P. Deck, Science **241**, 1176 (1988).
[9] H. Grunze and R. N. Lamb, Chem. Phys. Lett. **133**, 283 (1987).
[10] A. K. Chakraborty, H. T. Davis, and M. Tirrell, J. Polym. Sci. Part A: Polym. Chem. **28**, 3185 (1990).
[11] A. K. Chakraborty, J. S. Shaffer, and P. M. Adriani, Macromolecules **24**, 5226 (1991).
[12] J. S. Shaffer, A. K. Chakraborty, H. T. Davis, M. Tirrell, and J. L. Martins, J. Chem. Phys. **95**, 8616 (1991).
[13] A. K. Chakraborty, in *Proceedings of the International Conference on Polymer Solid Interfaces*, edited by J. J. Pireaux (Adam Hilger, Bristol, 1992), p. 3.
[14] A. K. Chakraborty and P. M. Adriani, Macromolecules **25**, 2470 (1992).
[15] P. G. de Gennes, in *New Trends in Physics and Physical Chemistry of Polymers*, edited by L. H. Lee (Plenum, New York, 1990).
[16] P. Frantz and S. Granick, Phys. Rev. Lett. **66**, 899 (1991).
[17] H. E. Johnson and S. Granick, Science **255**, 966 (1992).
[18] W. Barford and R. C. Ball, J. Chem. Soc. Faraday Trans. I **83**, 2515 (1987).
[19] A. R. Rossi, P. N. Sanda, B. D. Silverman, and P. S. Ho, Organometall. **6**, 580 (1987).
[20] B. D. Silverman, P. N. Sanda, J. G. Clabes, P. S. Ho, D. C. Hofer, and A. R. Rossi, J. Polym. Sci. Part A Polym. Chem. **26**, 1199 (1988).
[21] K. Kremer, J. Phys. **47**, 1269 (1986).
[22] R. G. Palmer, D. L. Stein, E. Abrahams, and P. W. Anderson, Phys. Rev. Lett. **53**, 958 (1984).
[23] J. S. Shaffer and A. K. Chakraborty, Macromolecules (in press).
[24] K. Konstandinidis, B. Thakkar, A. K. Chakraborty, R. Tannenbaum, J. F. Evans, L. W. Potts, and M. Tirrell, Langmuir **8**, 1307 (1992).
[25] G. H. Fredrickson and H. C. Andersen, Phys. Rev. Lett. **53**, 1244 (1984); J. Chem. Phys. **83**, 5822 (1985); G. H. Fredrickson and S. A. Brawer, *ibid.* **84**, 3351 (1986); G. H. Fredrickson, Annu. Rev. Phys. Chem. **39**, 149 (1988).
[26] J. L. Skinner, J. Chem. Phys. **79**, 1955 (1983).
[27] S. Butler and P. Harrowell, J. Chem. Phys. **95**, 4454 (1991).
[28] J. Reiter, J. Chem. Phys. **95**, 544 (1991).
[29] A. Silberberg, J. Phys. Chem. **66**, 1872 (1962).
[30] R. L. June, A. T. Bell, and D. N. Theodorou, J. Phys. Chem. **95**, 8866 (1991).
[31] R. Kohlrausch, Ann. Phys. (Leipzig) **12**, 393 (1847).
[32] K. L. Ngai, Comments Solid State Phys. **9**, 127 (1979); **9**, 141 (1980).
[33] R. G. Palmer, in *Heidelberg Colloquium on Spin Glasses*, edited by J. L. van Hemmen and I. Morgenstern (Springer, Berlin, 1983).
[34] S. Arrhenius, Z. Phys. Chem. (Leipzig) **4**, 226 (1889).
[35] H. Vogel, Phys. Z. **22**, 645 (1921).
[36] G. S. Fulcher, J. Am. Ceram. Soc. **8**, 339 (1925).
[37] S. A. Brawer, *Relaxation in Viscous Liquids and Glasses* (American Ceramic Society, Columbus, 1985).
[38] C. A. J. Hoeve, E. A. DiMarzio, and P. Peyser, J. Chem. Phys. **42**, 2558 (1965); C. Hoeve, J. Polym. Sci. Part C **30**, 361 (1970); **34**, 1 (1971).
[39] C. Truesdell, Ann. Mat. **46**, 144 (1945).